IPM motor rotor design by means of FEA-based multi-objective optimization

G. Pellegrino
Politecnico di Torino
C.so Duca degli Abruzzi, 24, Torino 10129, Italy
gianmario.pellegrino@polito.it

F. Cupertino
Politecnico di Bari
Via Orabona, 4, Bari 70125, Italy
cupertino@deemail.poliba.it

***Abstract* — The design optimization of IPM motors for wide speed ranges is pursued by means of a FEA-based multi-objective genetic algorithm (MOGA). Respect to previous works in the literature, the proposed approach evaluates the motor performance with a very limited number of simulations, making FEA optimization more attractive. The 3 goal functions (motor torque, torque ripple and flux weakening capability) are evaluated by means of 7 static FEA runs, that means nearly 20 seconds per tentative motor with a laptop computer. The paper is focused on the rotor design, since it is the most controversial part of IPM design and the most difficult to be modeled due to magnetic saturation. Three different approaches are presented: a fast one, based on 2-objective optimization, a hybrid one, based on 2-objective optimization and 3-objective refinement, and actual 3-objective optimization. The results presented here will be the base for future, more comprehensive optimization.**

I. INTRODUCTION

Interior Permanent Magnet (IPM) motors are particularly attractive in traction and spindle applications for their flux weakening capability, associated with a good torque density and high efficiency. One of the key issues in the IPM motors design is the definition of the rotor geometry, that is characterized by one or more flux barriers (or layers) with inset magnets. Many different geometries and related design approaches have been proposed in the literature throughout the last 20 years, based on analytical models, lumped parameter models, Finite Element Analysis (FEA) and optimization techniques [1-7]. To achieve a high speed range, the IPM motor must be properly designed: as clearly explained in [3]: the correct matching of permanent magnets (PM) flux and rotor magnetic saliency must be found, and magnetic saturation must be taken into account. High speed ranges are possible either with non salient rotors, like SPM with concentrated windings [8], or with multi layer IPM rotors with high saliency: the paper deals with the design of IPM motors with one ore more layers and distributed windings, where the willed speed range is obtained by means of a minimal quantity of PMs. This approach minimizes the cost of the PMs and many other side effects such as fault back-emf, short circuit current and flux-weakening current at no-load [4,9].

Due to the many degrees of freedom, there is no unique approach to the rotor design, in terms of layers number, layers shape and placement. Analytical modeling is effective for orienting the design but it is not sufficiently precise for forecasting the exact machine performance [4,7]. In many cases analytical models are associated to FEA [5,11]. Lumped parameter models are more accurate [6], but still they are not easy to be managed and require FEA to account for magnetic saturation effects: disregarding the saturation leads to extremely imprecise results [10]. Another important aspect that is difficult to be evaluated with simple models is the torque ripple, that can be very high in this kind of machines with poor design choices [12-14]. In other words, all the different design methods rely on finite element analysis (FEA), at least for the refinement stage.

The design optimization of an electric motor is a multi-objective optimization problem. Single and multi-objective optimization algorithms have been proposed for IPM motor design, associated to lumped parameter models of the motor [6,9,15-16]. FEA-based optimization has been rarely adopted to such motors because it requires a long computational time [17]. In some cases it has been applied to refine given designs [18], but there is no general design approach based on FEA optimization, like the one proposed in [19] for SPM motors, probably because of the complicate rotor geometry and the higher number of goals to be evaluated that include the maximum torque per ampere condition and the speed range evaluation besides torque density and machine cost. A three-objective design optimization based on FEA is proposed here, where the cost function is: maximum torque, minimum torque ripple, maximum constant power speed range (CPSR). The multi-objective algorithm outputs a Pareto front of non-inferior solutions from which the designer can select the most suitable one. In this first work, only the rotor geometry is optimized, since it is the most controversial point in IPM machines design. A multi-step static FEA is run over 7 positions for each tentative motor with an evaluation time around 20 s per individual. This excludes, in this work, the optimization of high speed losses, that need accurate transient simulations to be evaluated and could lead to different design solutions [20]. Future works based on the results presented here will include stator and rotor losses in the optimization, still with static FEA. Besides the 3-objective optimization (indicated as design 3 in the following), two faster methods (designs 1 and 2) based on successive partial optimization stages will be evaluated, and the results of the three different designs will be compared in terms of computational time and motor performance.

The goals of the paper are:

- to propose a FEA-based, 3-objective genetic optimization with a reasonable computational time thanks to the fast evaluation of rated torque, torque ripple and CPSR;
- to compare the results of the comprehensive 3-objective optimization (design 3) with faster runs with less individuals and less generations (designs 1 and 2);
- to draw general rules about the rotor design from the results of the optimization, in order to step ahead towards

978-1-4244-6392-3/10/$26.00 ©2010 IEEE

a more general optimization not limited to the rotor geometry.

II. IPM MOTOR DESIGN

At first, a simplified analysis is introduced for pointing out the goals of the design optimization. The approach is the one presented in [3] where the saliency ratio $\xi = L_q/L_d$ is used in the simplified motor model (1).

$$\begin{cases} \lambda_d = \lambda_m + L_d \cdot i_d \\ \lambda_q = \xi \cdot L_d \cdot i_q \end{cases} \tag{1}$$

Where λ_m is PM linked flux. The well known expression of torque (2) follows.

$$\frac{T}{\frac{3}{2}p} = \lambda_m \cdot i_q - (\xi - 1) \cdot L_d \cdot i_d i_q \tag{2}$$

With some manipulations, introducing the rated current i_0 and the phase angle γ defined in Fig. 1, expression (3) follows.

$$\frac{T}{\frac{3}{2}p} = \lambda_m \cdot i_0 \cdot cos\gamma - (\xi - 1) \cdot L_d \cdot i_0^2 \cdot \tfrac{1}{2} sin 2\gamma \tag{3}$$

The contributions of PM and rotor saliency to torque are evidenced in (2) and (3). Magnetic saturation is not taken into account in (1)-(3) and would lead to a more complicate model [5]: it is sufficient here to remark that the proper combination of PM flux and “saliency” flux must take into account magnetic saturation, as a limitation constraint.

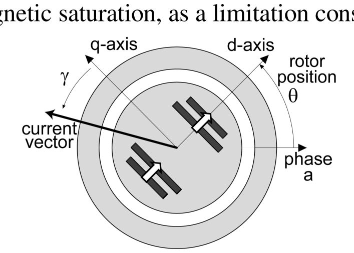

Figure 1. Schetch of the IPM motor, definition of the dq frame and the current phase angle γ.

A. Maximum torque

According to (3), the maximum torque for a given current is obtained by maximizing the two terms called PM torque and saliency torque. Due to magnetic saturation, the two terms can not be maximized separately and a tradeoff is necessary. It is general knowledge that the motors with the highest torque density are PM machines with poor saliency, such as isotropic SPM motors, where the PM flux is nearly the rated flux of the machine and the power factor is very high. On the opposite, the torque density of a pure reluctance motor (Synchronous Reluctance - SR) is lower than the one of a rare-earth based SPM motor, roughly by a factor 1.15÷1.25 depending on the pole pairs and design constraints [21]. To summarize: the maximization of the electromagnetic torque (2) alone would lead to a poorly salient motor, with big layers completely filled with high energy density magnets and no flux-weakening capability.

B. Constant Power Speed Range (CPSR)

The flux weakening capability of IPM machines has been clearly modeled in [3] by means of the λ_m, ξ plane: the optimal design curve is defined in such plane as the family of motors with infinite CPSR, that are those motors matching the well known condition (4).

$$-L_d \cdot i_0 = \lambda_m \tag{4}$$

In other words: a large CPRS can be achieved either with low saliency or high saliency motors by properly matched PM flux and rotor saliency but salient motors can achieve the same CPSR of non salient ones with less magnet volume and cost (lower λ_m and $L_d i_0$ terms, in per-units of the machine rated flux). Salient or not, a machine that satisfies the ideal condition (4), if properly designed, withstand a reduction of the rated torque to 70% if 100% is the torque obtained with a SPM motor with no flux weakening capability (CPSR = 1) [3]. This reduction is due to the rated power factor that is necessarily lower in machines with flux weakening capability. Real-world applications such as traction require a CPSR than is usually ≤ 5 and can have a higher power factor (78% with CPSR = 5 according to the linear model in [3]), but it must be kept in mind that CPSR>1 means a reduction of the obtainable rated torque.

Non-salient motors (SPM, single layer IPM) with concentrated windings can be designed to satisfy (4) and reach high CPSR values [8]. They are very compact due to the short end-connections, e.g. suitable for traction purposes [9]. Their main drawbacks are the high pole numbers (p = 5, 7 or multiples are typical), that further shrink the motor size but impose a high fundamental frequency (i.e. losses in the stator core and PMs), a high PM cost, dangerous back-emf values at high speed and high de-magnetizing currents, also at no-load. The analysis of this work will be devoted to rotor structures with inset magnets and distributed windings only, that are those machines with a reduced magnet cost, volume and related side-effects.

In the proposed optimization the infinite CPSR condition (4) will be pursued, because it is easy to be recognized with FEA. The L_d term strongly depends on the number of layers and scarcely on the layer heights, above a certain level. The L_q term (i.e. the saliency) depends on the rotor iron quantity, or basically on the overall width of the iron paths on the rotor. If the rotor iron paths are large enough, the L_q term is limited only by the stator iron saturation at rated current values. Generally speaking: more layers mean more saliency, unless enough iron is left for q-axis flux. The motor rated current i_0 in (4) depends on the thermal load. The λ_m term depends on the PM quality (residual flux density B_r) and volume.

C. Torque ripple

Torque ripple can be very high in IPM machines. In [11-12] it is shown that skewing the rotor by one stator pitch is not sufficient to smooth the torque completely. For a given number of stator slots, the number of rotor layers and their position at the airgap are the factors that mainly affect the torque ripple [12-14]. Some authors use equally spaced rotor layers and find the best combination with the stator slot number, while others suggest to move the layer positions and find minimum ripple geometries. In this work, the number of layers is given, and their geometry is optimized by the algorithm.

III. Genetic Multi-Objective Optimization (MOGA)

The design of electric motors is a multi-objective optimization problem: motor cost, compactness, efficiency and inverter size are the most common objectives to be optimized in the design of AC drives. The design objectives reveals conflicting interests and the most preferable trade-off is not a-priori known and difficult to be found during the design procedure. The most commonly adopted strategy to solve multi-objective optimization problems is to define an aggregated cost function expressed as a weighted sum of indexes related to the various goals and then implement a single objective algorithm [24]. This approach is simple, requires lower computational cost and usually gives a single solution with no extra design effort. Unfortunately, the formulation of the aggregated cost function stiffly influences the results of the optimization and a successful result requires an a-priori knowledge of the optimal trade-off among the optimization goals. As an alternative approach multi-objective optimization algorithms can be adopted [22]. Such algorithms search for a set of possible solutions according the well known Pareto dominance criterion. Each candidate solution of the problem is associated with a vector-valued cost function. Each element of the cost function vector represent a single objective to be minimized. A possible solution is not dominated and belongs to the Pareto front if no other solution has all the cost function elements equal or (at least one) lower. Generating the Pareto set can be computationally expensive and is often infeasible using exact methods. The use of stochastic search strategies such as evolutionary algorithms is an attempt to find a good approximation of the Pareto set, with a reasonable computational effort. Genetic algorithms [23] are effective methods in complex noisy environments and have been adopted here to approximate the Pareto front and shorten the automatic design procedure [25]. Once the Pareto front is obtained the motor designer can select the best compromise among the different goals knowing how much a single objective has to be penalized to improve another one. Thus the human decision is after the automatic solution and not before, and the best compromise can be reasonably obtained for a wider range of problems.

The convergence of genetic-based optimization methods relies on the proper choice of population size and evolution generations that must be tuned according to the problem complexity [24-25]. For this reason it is very important that the functional evaluation is computationally light to permit a high number of iterations in a reasonable time. Computation time is the main limitation of FEA-based optimization, particularly for machines with such a complicate geometry and output requirements (average torque, torque ripple, flux weakening capabilities).

A. *Problem statement*

The stator geometry is completely defined. The number of turns is preliminary chosen and can be adapted later for modifying the rated current and voltage of the optimal machine. The rated current i_0 is calculated according to the accepted thermal load, expressed in stator Joule losses. The acceptable losses depend on the motor size and type of cooling.

The rotor geometry is defined in Fig. 2 for a 2 pole-pairs, 3 layers IPM motor. Bonded magnets are adopted for simplicity. Nevertheless, the validity of the model can be easily extended to sintered magnets machines, as it will be demonstrated in the final paper: the bonded magnet that fills the layers completely can be substituted with smaller sintered magnet blocks that partially fill the layers. The localized stronger magnets tend to saturate the iron in their neighborhoods more than the optimized bonded ones: as will be shown in the following, optimized machines have wide rotor iron paths and can withstand the magnets substitution with no particular loss of performance in most of cases. The laminations ribs at airgap are of a fixed width that depends on the bore diameter and to punching limits. The radial ribs are calculated automatically for withstanding a centrifugal stress of 180N/mm^2 at overspeed. Let n_{lay} be the number of rotor layers: the set of parameters to be optimized is composed by:

- the $\Delta\alpha_j$ angles ($j = 1 \div n_{lay}$), that define the layer positions at the airgap;
- the layer heights hc_j , $j = 1 \div n_{lay}$;
- the residual flux density of the permanent magnets B_r;
- the current phase angle γ.

The size of the vector of parameters ($2 \cdot n_{lay} + 2$) varies with the number of layers. As said machines with more layers give a better performance, but they are also more difficult to be manufactured and then more expensive, thus the number of layers is a preliminary choice of the designer. The 3-layer rotor has been chosen as an example.

A set of the above parameters defines the machine geometry. To evaluate the motor performance the current angle is also optimized as explained in the next subsection.

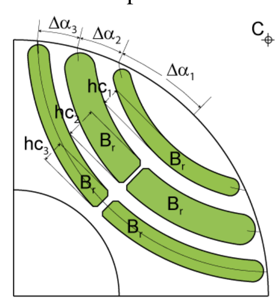

Figure 2. Rotor geometry with 3 layers: the $\Delta\alpha_j$ angles define the layer angular positions, hc_j are the layer heights and B_r defines the PM quality .

B. *Maximum torque current angle γ_{MTPA}.*

The rated torque is obtained for the maximum torque per Ampere (MTPA) current angle that is unknown and can vary from 0 for an isotropic machine to over 45° for a very salient and saturated machine. The knowledge of γ_{MTPA} is needed for calculating the rated torque of the tentative motors. For evaluating such angle multiple simulations for different γ values might be required but they would be time consuming. For this reasons γ is included in the optimization process: each tentative motor is simulated for only one current angle selected by the MOGA, and it can be shown that for all the machines on the Pareto front the correct γ_{MTPA} has been found by the algorithm.

C. *Evaluation of torque ripple.*

For evaluating the torque ripple 6 static simulations are run along one stator slot pitch and the standard deviation of the torque waveform is calculated. Six positions is a rough approach that is focused on eliminating the ripple component at the stator slot periodicity. Higher and lower order ripple components can survive to the optimization process but they are normally less critical.

D. *Evaluation of CPSR.*

The CPSR is not calculated because it would require a longer machine identification as for γ_{MTPA}. The zero d-flux condition (4) is pursued by means of a single static simulation with $i_d = -i_0$ ($\gamma = 90°$). The optimized machines are ranked according to their distance from the ideal condition (4) in the Pareto front and the CPSR follows monotonically.

All considered, the functional evaluation for calculating torque, ripple and CPSR of each tentative motor consist of 7 static FEA runs, that means 20 seconds on a standard laptop computer (Intel Centrino T7200 @ 2 GHz).

E. *Boundaries of the input parameters.*

The domain of the input parameters is defined as follows. Since the torque ripple depends combination of stator and rotor "slot" pitches, the range of the $\Delta\alpha_j$ angles must depend on the stator pitch value. In particular the $\Delta\alpha_j$ can span from one half to two times the stator slot pitch. A specific definition is needed for $\Delta\alpha_1$ that can span from zero to the maximum value (5) that corresponds to all the other angles at one half of the stator pitch.

$$\Delta\alpha_1 \le \frac{1}{p}\cdot\left[90-\frac{1}{2}\cdot\frac{360}{n_s}\cdot\left(n_{lay}-0.5\right)\right] \qquad (5)$$

Where $\Delta\alpha_1$ is expressed in mechanical degrees, p is the number of pole-pairs, n_s is the number of stator slots per pole-pair, $360/n_s$ is the stator pitch in electrical degrees.

Once the $\Delta\alpha_j$ are defined, the layer heights hc_j can span from 0 to 1 in per-unit of the space available according to the layer positions. Minimum iron and minimum layer heights are guaranteed, according to manufacturing requirements.

The residual flux density B_r can vary from 0.2T to 1.0T and the current phase angle γ varies from 0° to 80°.

IV. DESIGN OPTIMIZATION OF A 3 LAYER IPM MOTOR

Three different designs are presented, from the fastest one to the more accurate. The 3-objective accurate optimization (Design 3) will be used as the reference solution for evaluating the results of the other two methods.

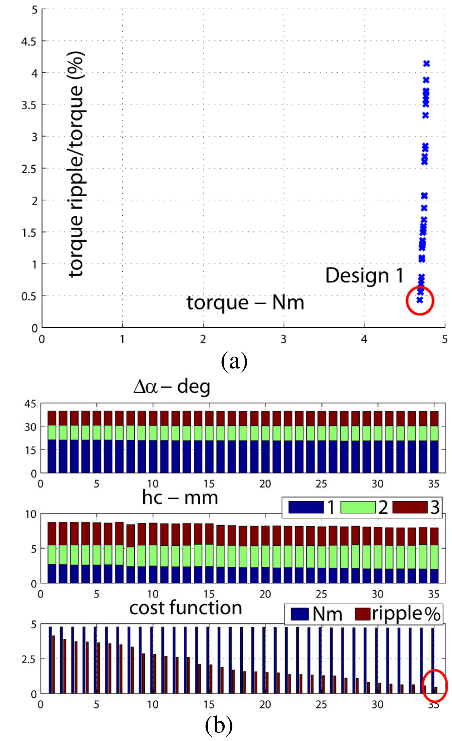

Figure 3. Design 1: results of torque-ripple optimization with B_r = 1.0T and selection of the minimum ripple machine. a) Pareto front; b) motor geometry, torque and ripple of the 35 individuals of the Pareto front.

A. *Design 1: torque-ripple optimization and B_r tuning.*

The 2-objective optimization of torque and ripple is performed with a fixed B_r = 1.0T giving out the two-dimensional Pareto front of Fig. 3a. All the motors on the front have nearly the same torque, thus the minimum ripple motor is selected as the best one (number 35 in Fig. 3b). The power Vs speed curve of solution 35 is reported in Fig. 4: with B_r = 1.0 T the motor has no flux weakening capability, because of the very high PM flux that can not be counterbalanced by the $L_d i_0$ term. The machine behaves like a SPM motor from this point of view. The CPSR can be enhanced by varying the magnets properties (B_r) manually. As Fig. 4 explains, for the motor under test a quasi-ideal CPSR is obtained by posing B_r = 0.3T. Once the magnets are modified, the torque and ripple of this machine are not optimal anymore: nevertheless it will be shown in the following (Fig. 7) that they have acceptable values with respect to the best solution of design 3. The choice of B_r = 1.0T as starting value has been purposely made to demonstrate the robustness of this first design method with a tentative value that is far from the final value of B_r = 0.3T: once the torque ripple has been optimized, even large variations of the magnets properties produce machines with rather low ripple. The computational time required by the 2-objective optimization is 25 hours (60 individuals, 50 generations).

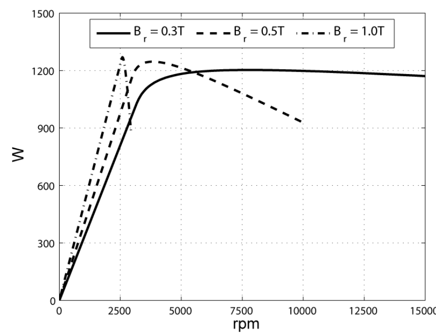

Figure 4. Design 1: power profiles with Br = 1T , Br = 0.5T and Br = 0.3T respectively.

B. Design 2: torque-ripple optimization plus fast torque-ripple-CPSR optimization.

In Fig. 3b the $\Delta\alpha$ and hc values for all the machines of the front are reported showing very little differences from the first to the last machine, in particular the layers positions are practically the same for all the machines. A 3-objective optimization has been run with B_r variable and the $\Delta\alpha$ bounds restricted to ±5% of the values of Design 1. Due to the restricted domain of the inputs, the 3-objective optimization can be performed with a restricted number of iterations and takes nearly 40 hours (100 individuals, 50 generations). The selected machine is evidenced in Fig. 5 as Design 2. Torque and power curves are reported in Fig. 7 and Fig. 8 respectively.

C. Design 3: torque-ripple-CPSR optimization

A 3-objective optimization has been performed in the whole research space with 200 individuals and 80 generations. The computation time was 130 hours, that is approximately twice the time needed for Design 1 plus Design 2.

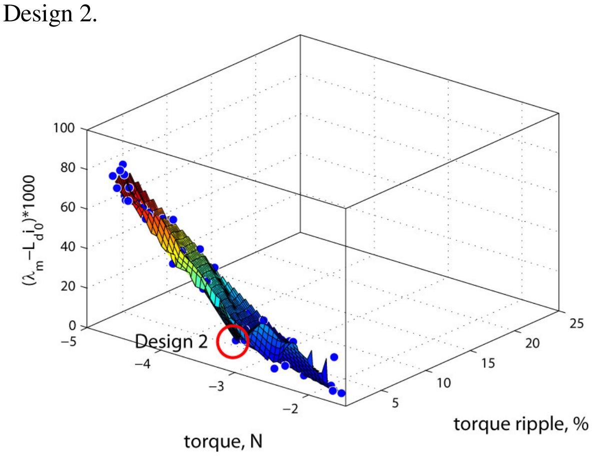

Figure 5. Design 2: Pareto front of torque-ripple-CPSR optimization based on the 2-objective optimization of design 1.

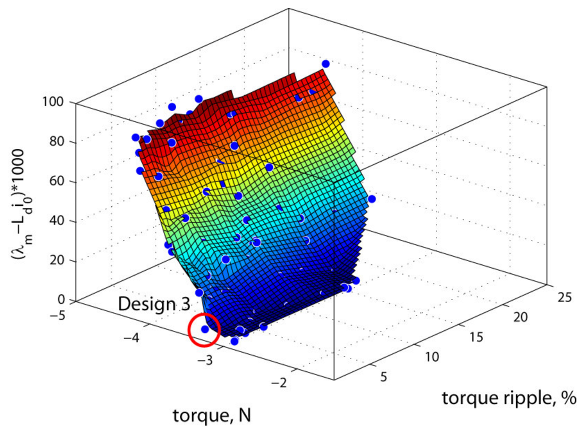

Figure 6. Design 3: Pareto front of torque-ripple-CPSR optimization.

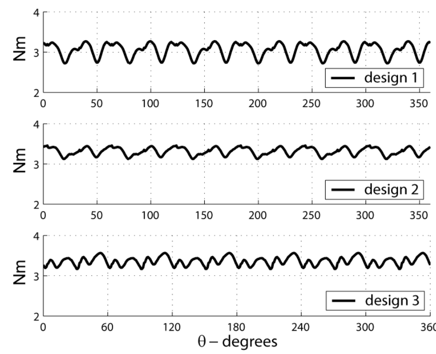

Figure 7. Rated torque comparison. top: design 1, middle: design 2, bottom: design 3.

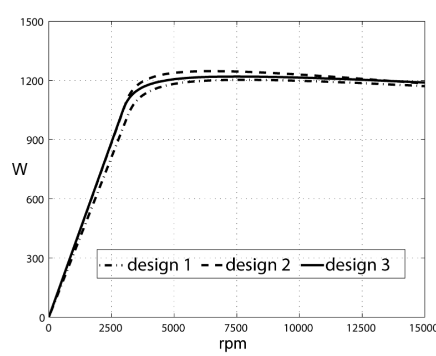

Figure 8. Power Vs speed characteristics of the 3 resulting machines.

D. Results of the analysis.

The torque waveforms of the designs in rated conditions are reported in Fig. 7. Design 2 and Design 3 give the same average torque (3.3 Nm) and comparable ripple values (3%), with different harmonic contents. As said, Design 1 gives a lower torque and a higher ripple since torque and ripple have been optimized with B_r = 1 T while the final design has B_r = 0.3T. The lower performance is justified by the short computation time required by Design 1, and it is not critical, as can be also evinced by comparing the power profiles of the three motors in Fig. 8 that are very similar.

Some key-observations about the results of the analysis can be done:

- The Pareto fronts of Figs. 5 and 6 put in evidence that the motor torque and CPSR are two competing goals, in accordance with the analysis of section II.B.
- On the opposite, there is no competition between torque ripple and the other two goals of the optimization (Figs. 3a, 5, 6): solutions with high torque can have either high or low ripple and the same can be said for the solutions with high CPSR.
- The torque reduction related to a high CPSR, introduced in section II.B, is evidenced by Fig. 4, where the same motor has a low CPSR when B_r = 1 T due to the high PM flux and a high CPSR when the PM flux is matched correctly to the motor saliency (with B_r = 0.3 T).
- The value B_r = 0.3T has been chosen manually and the power curve of design 1 matches the infinite speed condition (4) only partially. A finer tuning of the B_r value (around 0.35T) would have been required in order to match (4) exactly. This justifies the lower torque of Design 1 with respect to Designs 2 and 3 evidenced in Figs. 7-8.
- A confirmation of that is given by the performance of Design 2, that has a similar rotor geometry (Figs. 9-10) but a higher B_r = 0.38 T that results in a higher torque with nearly the same CPSR. This means that in design 1 $\lambda_m - L_d i_0 < 0$ while in design 2 $\lambda_m - L_d i_0 > 0$ that is a better compromise for real-world designs.
- With real-world bonded magnets and actual magnetization direction (that is not uniform as in FEA), the three curves can withstand little modifications, but all the three designs are comparable in terms of performance.
- With sintered magnets the areas of the magnets must be reduced with the inverse proportion of the magnets properties.
- Design 3 has a lower PM quantity and a more robust rotor lamination with respect to designs 1 and 2. This means that the layer positions that minimize the torque ripple are not unique and depend on the adopted magnets. In particular layer one (the smallest one) is in a different position, while layer 2 and 3 have practically the same positions for the 3 designs. All considered, the layers positions that are optimal with B_r = 1T are still good for ripple with weaker magnets (Design 1 and 2).
- If the torque-ripple optimization of design 1 was run with a weaker magnet (e.g. 0.5T) machines 1 and 2 would have been more similar to machine 3. As said, the value B_r = 1.0 T was chosen on purpose.
- Design 3 has a better saliency due to a larger flux path and this is the reason of the lower PM quantity for achieving the same power profile, according to subsection II.B.

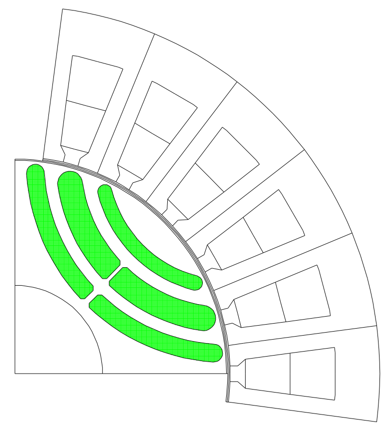

Figure 9. Design 1, from torque-ripple optimization and manula tuning of CPSR by means of B_r. Br is 0.3T.

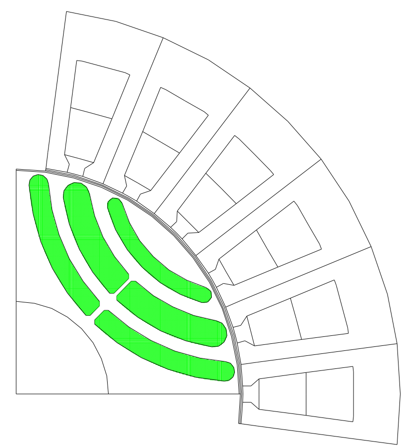

Figure 10. Design 2, from torque-ripple-CPSR optimization based on the $\Delta\alpha$ angles derived from Design 1. Br is 0.38T.

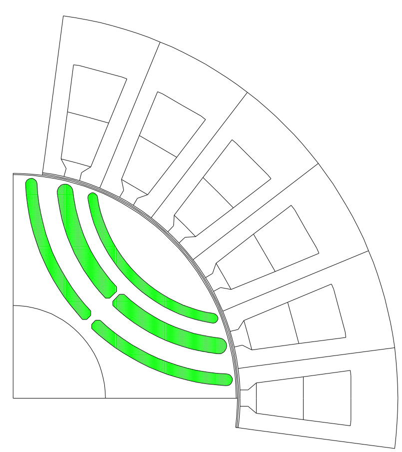

Figure 11. Design 3, from torque-ripple-CPSR optimization in the whole search region. Br is 0.41 T.

V. CONCLUSIONS

The design optimization of multi-layer IPM motors by means of multi-objective genetic algorithm has been proposed and tested. The MOGA runs a FEA model of the motor, capable of evaluating the three cost functions (torque, ripple, constant power speed range) with a minimal number of static simulations. Three design methods have been proposed and tested on a 3-layer rotor for home appliances. It has been shown that acceptable machines can be achieved with a relatively fast 2-objective optimization (torque-ripple) and manual tuning of the PMs quality. In particular, the CPSR can be easily augmented or reduced for any machine by modifying the quality of the PMs (or, in proportion, the volumes). With the complete 3-objective optimization a better machine is obtained, in terms of minimum ripple and minimum magnets quantity. Future works will proceed in two parallel directions: on one hand the simplification of the problem statement in order to introduce new optimization inputs (stator geometry, pole pairs) and cost functions (core losses), on the other hand the improvement of computational devices, by means of parallel computing and multi-core machines.

ACKNOWLEDGMENT

This research is being conducted in the frame of project TISCOM, supported by Regione Puglia, code DM01 .

APPENDIX – MOTOR DATA.

The motor under optimization is for home appliances. The main input data are: stator diameter 101 mm, bore diameter 58.5 mm, airgap 0.5 mm, 2 pole-pairs, 24 slots. The steel ribs at the rotor airgap are 0.4 mm wide. Maximum speed is 15000 rpm. The copper loss of the active part is 135W that corresponds to 5.35A (pk) at 115°C. The motor rated voltage is 162V (phase, pk).

REFERENCES

[1] T. M. Jahns, G. B. Kliman, and T. W. Neumann, “Interior permanent magnet synchronous motors for adjustable-speed drives”, IEEE Trans. Ind. Appl., vol. IA-22, pp. 738-747, July/Aug. 1986.

[2] R. Schiferl,T.A. Lipo, “Power capability of Salient pole P.M. synchronous motors in variable speed drive”, Conf. Record. of IEEE-IAS annual meeting 1988, pp: 23-31.

[3] W. Soong and T. J. E. Miller, “Field weakening performance of brushless synchronousAC motor drives,” Proc. IEE—Elect. Power Appl., vol. 141, no. 6, pp. 331–340, Nov. 1994.

[4] A. Fratta, A. Vagati, F. Villata, “Design criteria of an IPM machine suitable for field-weakening operation”, International Conference on Electrical Machines, ICEM90, Boston 1990, U.S.A., pp: 1059-1065.

[5] N. Bianchi and S. Bolognani, "Magnetic models of saturated interior permanent magnet motors based on finite element analysis" in Proc. of 1998 IEEE Ind. Appl. Soc. Annual Meeting, vol. 1, pp. 27-34, Oct 1998.

[6] E.C. Lovelace, “Optimization of a Magnetically Saturable Interior PM Synchronous Machine Drive”, PhD Thesis, Dept. of Elec. Eng. & Comp. Sci., MIT, 2000.

[7] N. Bianchi, S. Bolognani, A. Consoli, T.M. Jahns, R.D. Lorenz, E.C. Lovelace, S. Morimoto, A. Vagati, “Design, analysis, and control of interior PM synchronous machines,” in Proc. IEEE IAS Tutorial Course Notes, IAS Annu. Meeting, N. Bianchi and T. M. Jahns, Eds. Seattle, WA: CLEUP, Oct. 3, 2004.

[8] EL-Refaie, A.M.; Jahns, T.M., "Optimal flux weakening in surface PM machines using fractional-slot concentrated windings," *Industry Applications, IEEE Transactions on* , vol.41, no.3, pp. 790-800, May-June 2005

[9] El-Refaie, A.M.; Jahns, T.M., "Comparison of synchronous PM machine types for wide constant-power speed range operation," *Industry Applications Conference, 2005. Fourtieth IAS Annual Meeting. Conference Record of the 2005* , vol.2, no., pp. 1015-1022 Vol. 2, 2-6 Oct. 2005.

[10] Lovelace, E.C.; Jahns, T.M.; Lang, J.H., "Impact of saturation and inverter cost on interior PM synchronous machine drive optimization," *Industry Applications, IEEE Transactions on* , vol.36, no.3, pp.723-729, May/Jun 2000.

[11] G. Qi, J. T. Chen, Z. Q. Zhu, D. Howe, L. B. Zhou, C. L. Gu, “Influence of skew and cross-coupling on flux-weakening performance of PM brushless AC machines” IEEE Trans. Magnetics, vol.45, no.5, pp.2110-2117, May 2009.

[12] Vagati, A.; Pastorelli, M.; Francheschini, G.; Petrache, S.C., "Design of low-torque-ripple synchronous reluctance motors," *Industry Applications, IEEE Transactions on* , vol.34, no.4, pp.758-765, Jul/Aug 1998

[13] Jahns, T.M.; Soong, W.L., "Torque Ripple Reduction in Interior Permanent Magnet Synchronous Machines Using the Principle of Mutual Harmonics Exclusion," *Industry Applications Conference, 2007. 42nd IAS Annual Meeting. Conference Record of the 2007 IEEE* , vol., no., pp.558-565, 23-27 Sept. 2007

[14] Bianchi, N.; Bolognani, S.; Bon, D.; Dai Pre, M., "Rotor Flux-Barrier Design for Torque Ripple Reduction in Synchronous Reluctance and PM-Assisted Synchronous Reluctance Motors," *Industry Applications, IEEE Transactions on* , vol.45, no.3, pp.921-928, May-june 2009.

[15] Sibande, S.E.; Kamper, M.J.; Wang, R.; Rakgati, E.T., "Optimal design of a PM-assisted rotor of a 110 kW reluctance synchronous machine," *AFRICON, 2004. 7th AFRICON Conference in Africa* , vol.2, no., pp. 793-797 Vol.2, 15-17 Sept. 2004

[16] Raminosoa, T.; Rasoanarivo, I.; Sargos, F.-M.; Andriamalala, R.N., "Constrained Optimization of High Power Synchronous Reluctance Motor Using Non Linear Reluctance Network Modeling," *Industry Applications Conference, 2006. 41st IAS Annual Meeting. Conference Record of the 2006 IEEE* , vol.3, no., pp.1201-1208, 8-12 Oct. 2006

[17] Wen Ouyang; Zarko, D.; Lipo, T.A., "Permanent Magnet Machine Design Practice and Optimization," *Industry Applications Conference, 2006. 41st IAS Annual Meeting. Conference Record of the 2006 IEEE* , vol.4, no., pp.1905-1911, 8-12 Oct. 2006

[18] Yamazaki, Katsumi; Kanou, Yuji; Fukushima, Yu; Ohki, Shunji; Nezu, Akira; Ikemi, Takeshi; Mizokami, Ryouichi, "Reduction of magnet eddy current loss in interior permanent magnet motors with concentrated windings," *Energy Conversion Congress and Exposition, 2009. ECCE. IEEE* , vol., no., pp.3963-3969, 20-24 Sept. 2009

[19] Bianchi, N.; Bolognani, S., "Design optimisation of electric motors by genetic algorithms," *Electric Power Applications, IEE Proceedings -* , vol.145, no.5, pp.475-483, Sep 1998.

[20] Pellegrino, G.; Guglielmi, P.; Vagati, A.; Villata, F., "Core loss and torque ripple in IPM machines: dedicated modeling and design trade off," *Energy Conversion Congress and Exposition, 2009. ECCE. IEEE* , vol., no., pp.1911-1918, 20-24 Sept. 2009

[21] A. Vagati, A. Fratta, G. Franceschini, P. Rosso, “AC Motors for High-Performance Drives: A Design-Based Comparison”, *Industry Applications, IEEE Transactions on* , vol.32, no.5, pp.1211-1219, Sept/Oct 1996.

[22] K. Deb, “Multi-objective optimization using evolutionary algorithms”, Wiley-Interscience Series in Systems and Optimization, 2001.

[23] David E. Goldberg “Genetic Algorithms in Search, Optimization and Machine Learning”, Addison Wesley, 1989.

[24] F. Cupertino, E. Mininno, D. Naso, B. Turchiano, and L. Salvatore: “On-line Genetic Design of Anti-Windup Unstructured Controllers for Electric Drives with Variable Load”, IEEE Trans. on Evolutionary Computation Vol. 8, No 4, 2004, pp.347-364.

[25] Kalyanmoy Deb, Amrit Pratap, Sameer Agarwal, T Meyarivan “A fast and elitist multiobjective genetic algorithm: NSGA-II”, IEEE Trans. on Evolutionary Computation, Vol. 6, n. 2, pp. 182-197, 2002.